

Article

Basalt from the Extinct Spreading Center in the West Philippine Basin: New Geochemical Results and Their Petrologic and Tectonic Implications

Zhengxin Yin ^{1,2}, Weiping Wang ^{1,2,*}, Liang Chen ^{1,2,*}, Zhengyuan Li ^{1,2}, Qiang Liu ^{1,2} and Anyuan Xie ^{1,2}

- ¹ South China Sea Marine Survey and Technology Center, State Oceanic Administration, Guangzhou 510300, China; yinzhengxin@smst.gz.cn (Z.Y.); lizhengyuan@smst.gz.cn (Z.L.); liuqiang@smst.gz.cn (Q.L.); xieanyuan@smst.gz.cn (A.X.)
- ² Key Laboratory of Marine Environmental Survey Technology and Application, Ministry of Natural Resources, Guangzhou 510300, China
- * Correspondence: wangweiping@smst.gz.cn (W.W.); chenliang@smst.gz.cn (L.C.)

Abstract: We present geological, bulk-rock geochemical and Sr–Nd–Hf isotopic data for mafic rocks from the West Philippine Basin (WPB). These mafic rocks comprise pillow basalts characterized by a vesicular structure. The mid-ocean ridge basalt (MORB)-normalized trace element patterns of basalts from the study area display depletions in Nb. In addition, the chondrite-normalized lanthanide patterns of basalts from the WPB are characterized by significant depletions in the light lanthanides and nearly flat Eu to Lu segments. The investigated rocks have initial ⁸⁷Sr/⁸⁶Sr ratios (⁸⁷Sr/⁸⁶Sr(i)) of 0.703339–0.703455 and high ε_{Nd}(t) values (8.0 to 8.7). Furthermore, basalts from the WPB have ¹⁷⁶Hf/¹⁷⁷Hf ratios that range from 0.28318 to 0.28321 and high ε_{Hf}(t) from 15.2 to 16.3. Semi-quantitative modeling demonstrates that the parental melts of basalts from the study area were derived by ~20% adiabatic decompression melting of a rising spinel-bearing peridotite source. The Sr–Nd–Hf isotopic compositions of basalts from the WPB indicate that their parental magmas were derived from an upper mantle reservoir possessing the so-called Indian-type isotopic anomaly. Interpretation of the isotopic data suggests that the inferred mantle source was most likely influenced by minor inputs of a sediment melt derived from a downgoing lithospheric slab. Collectively, the petrographic and geochemical characteristics of basalts from the study area are analogous to those of mafic rocks with a back-arc basin (BAB)-like affinity. As such, the petrogenesis of basalts from the WPB can be linked to upwelling of an Indian-type mantle source due to lithospheric slab subduction that was followed by back-arc spreading.



Citation: Yin, Z.; Wang, W.; Chen, L.; Li, Z.; Liu, Q.; Xie, A. Basalt from the Extinct Spreading Center in the West Philippine Basin: New Geochemical Results and Their Petrologic and Tectonic Implications. *Minerals* **2021**, *11*, 1277. <https://doi.org/10.3390/min1111277>

Academic Editors: Francisco J. González, A. Filipa A. Marques and Blanca Rincón-Tomás

Received: 19 October 2021

Accepted: 15 November 2021

Published: 18 November 2021

Publisher's Note: MDPI stays neutral with regard to jurisdictional claims in published maps and institutional affiliations.



Copyright: © 2021 by the authors. Licensee MDPI, Basel, Switzerland. This article is an open access article distributed under the terms and conditions of the Creative Commons Attribution (CC BY) license (<https://creativecommons.org/licenses/by/4.0/>).

Keywords: basalt; geochemistry; isotopes; West Philippine Basin

1. Introduction and Rationale of the Study

The Philippine Sea Plate (PSP) is a significant element of the large-scale lithospheric organization of our planet that has been affecting the geodynamic evolution of the Western Pacific area since the Mesozoic eon. The PSP is primarily composed of an oceanic lithosphere of mid-ocean ridge (MOR) to suprasubduction zone (SSZ) affinity of the Early Cretaceous to Cenozoic age. An important compositional aspect of the mafic rocks that have been recovered from the PSP is that they show a wide range of geochemical affinities, varying from normal mid-ocean ridge basalts (N-MORB) to enriched MORB (E-MORB) and oceanic island basalts (OIB) [1–12]. In addition, the isotopic characteristics of basalts from the PSP suggest that magmatism in this area tapped an upper mantle region that was compositionally different from that underneath the spreading ridges of the Pacific Ocean.

The West Philippine Basin (WPB) is the oldest and probably the most well-studied among the (Western Pacific) marginal basins of the PSP. The origin of basalts from the WPB has raised significant controversy among geoscientists the last few decades. Three

competing hypotheses have been proposed to theoretically explain the origin of the basalts from the WPB. The first scenario invokes that the WPB is a fragment of a trapped oceanic spreading ridge of the New Guinea–Pacific lithosphere [13]. The second model interprets the WPB as a back-arc basin (BAB) that was formed among two SSZ [14,15]. The third hypothesis views the development of the WPB as influenced by both back-arc spreading and a mantle plume [10–12,16,17]. All these models highlight the need for more precise data on the petrologic nature of basalts from the WPB to determine the geological origin of this specific basin of the PSP.

Herein, a detailed report is provided on the petrographic, geochemical, and Sr–Nd–Hf isotopic data for the mafic rocks we recovered from the WPB. These data integrated with those of previous investigations provide invaluable insights into the geological evolution of the WPB and can be used to create a more sophisticated hypothesis for a reconceptualization of the tectono-magmatic and spreading history of the western part of the PSP.

2. Geological Setting

The Philippine Sea is one of the largest marginal basins of the Pacific Ocean. It is subdivided into three domains on the basis of geomorphology, namely: the Paleocene–Eocene West Philippine Basin (WPB) and the Daito Ridge (DR) Province in the west, the Oligocene–Miocene Shikoku Basin (SB) and the Parece Vela Basin (PVB) in the east, and the Izu–Bonin–Mariana (IBM) island arc further to the east (Figure 1a). The WPB is the oldest basin in the Philippine Sea Plate (PSP). Magnetic anomaly estimations support that the WPB opened in a NE–SW/N–S direction between ~65 and 35 Ma by spreading along an extinct spreading center marked by the Central Basin Fault (CBF) [15,18], a 1000-km-long NW–SE-oriented ridge cut by a system of N–S-trending fracture zones (Figure 1a). At the present time, the WPB is subducting beneath the eastern side of the Ryukyu–Taiwan–Philippine arcs and controls the volcanic activity there (Figure 1a) [19]. On the east, it is bounded by the N–S-trending Kyushu–Palau Ridge, a Paleocene–Eocene remnant structure of a proto-IBM island arc (Figure 1a).

Despite detailed petrologic and geophysical explorations during the Deep Sea Drilling Project (DSDP), the geochemical and geotectonic evolutions of the WPB remain largely enigmatic. Antagonistic models predict that the WPB is an old fragment of ocean lithosphere trapped in the PSP [20], part of a back-arc basin (BAB) linked to the evolution of the proto-IBM arc [21,22], or (3) a mid-ocean ridge (MOR) formed by a hotspot that migrated beneath the ocean floor [3]. Basalts recovered from the seafloor of the WPB have both mid-ocean ridge basalt (MORB)- and oceanic island basalt (OIB)-like characteristics [1,4,10–12]. Nevertheless, among the OIB-like volcanic rocks of the WPB, only a few are related to seamounts (i.e., Benham Rise). Therefore, the compositional characters of basalts from the WPB cannot be explained in a simple way.

West Philippine Basin studies are also complicated by the fact that all rock outcrops are ~5 to 6 km below the surface of the water, with those of the CBF fossil spreading axial valley at a depth of ~8 km. The origin and structure of the CBF remain unresolved. Submarine topographic observations have shown that the CBF is a segmented spreading ridge with a morphology analogous to that of a (slow) spreading environment with a non-transform offset, a nodal deep, and an inside corner high [7]. On the contrary, the geochemical affinity of basalts from the CBF suggests that they were produced in a BAB setting. These contrasting data confirm that the CBF has a rather complicated geological history.

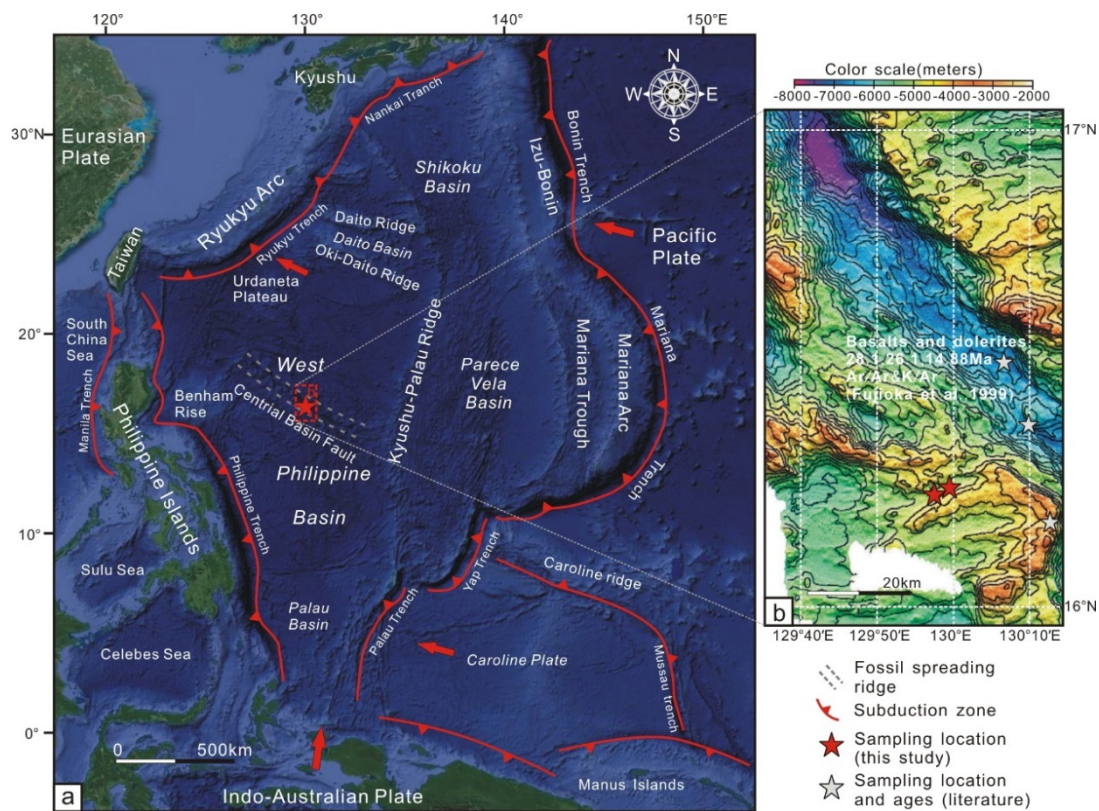


Figure 1. (a) Schematic tectonic framework of the Philippine Plate showing major tectonic subdivisions (modified after Reference [18]). (b) Geomorphological–bathymetric map illustrating the survey area (modified after Reference [22]). A gray star represents previously dated pillow lava [7]. The sample sites for this work are also marked by a red star.

3. Sampling and Geological Observations

3.1. Sampling Strategy

A research cruise was organized to collect bathymetric and geological data along the CBF. Sampling was done by dragnet over a single cruise during the summer season of 2019. All rock samples ($N = 10$) came from water depths of ~5 to 6 km and were collected from different sites of a relatively broad region (16.25° N; 129.99° E) in the central part of the CBF (Figure 1b). A small number of strongly altered samples ($N = 2$) were excluded from our investigation, as they could not be used for geochemical analysis. We note that the study area has been the subject of detailed sampling in the past [7]. However, we decided to focus on this area again in order to compare the results of our research with those of previous studies. Sampling was undertaken to delineate the petrologic aspects of the mafic rocks (by assessing their complexity at the m to tens of m scales) and determine if the magmatism in the study area was characterized by any significant geochemical and isotopic variations.

Our bathymetric observations show that the depth does not increase systematically as we move away from the axis of the CBF. As such, the bathymetric profile across the CBF does not fit that of a typical spreading environment. In addition, our structural observations indicate the occurrence of a set of E–W-trending lineations along the CBF interrupted by a group of N–S-oriented fault zones. This results in a roughly NW to SE crisscross pattern along the CBF. The central part of the CBF is nearly flat and is covered by a thick layer of bathypelagic sediments. Furthermore, the off-axis area shows an E–W set of fracture zones, suggesting that the spreading was oblique to the direction of the rift process.

3.2. Petrography

Most of the rock samples collected from the seafloor of the WPB show quite similar lithological characteristics at the mesoscopic scale. As such, their petrographic features are described together, emphasizing their most striking differences when necessary.

All the samples exhibit a grey to light green color, displaying a pervasive isotropic, aphanitic igneous fabric indicative of their volcanic origin (Figure 2a). Most of the investigated rock samples are vesiculated (Figure 2b). The vesicles are thought to represent former gas bubbles. They are large (<3 mm in diameter) and globular, occupying less than 10–15% of the total volume of a single hand specimen. In a few samples, there is evidence of gas bubble nucleation and coalescence due to strain localization in response to discontinuous lava flow. A small number of vesicular cavities in each rock sample may be lined or filled with calcite or fibrous zeolite group minerals. Some specimens have (~1.0 cm thick) glassy outer margins (Figure 2b) occasionally accompanied by weak radial jointing due to spallation during cooling. These rock samples most likely represent pillow lava fragments. Although most of the investigated mafic rock samples have preserved their original volcanic features, some of them display ~1 to 2 cm thick post-eruption alteration-related selvages or may be coated with manganese- and/or zeolite-rich crusts.

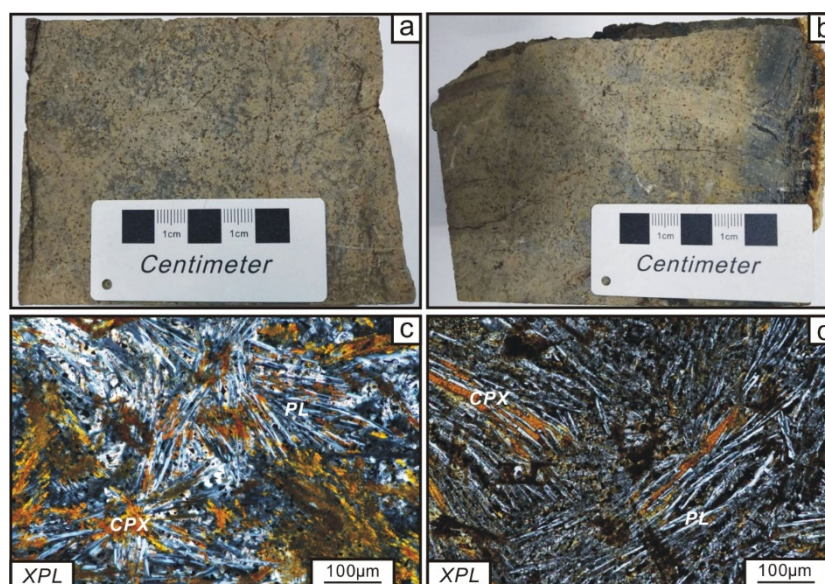


Figure 2. Macroscopic photos illustrating a hand specimen of a mafic rock collected from CBF in WPB with (a) a pervasive isotropic, aphanitic (volcanic) fabric or (b) a vesicular structure, with a glassy outer margin. Photomicrographs of basalts with a (c) spherulitic texture or (d) trachytic texture. Abbreviations (in alphabetical order): CPX, clinopyroxene and PL, plagioclase.

Three polished thin sections were prepared from each of the 8 rock samples collected for the purpose of our study. All rock sections were investigated under transmitted and reflected light, using an Olympus BX53M optical microscope at the Key Laboratory of Marine Environmental Survey Technology and Application, Ministry of Natural Resources, Guangzhou (China).

All rock samples showed a high proportion of crystals (<75–80% modal) over volcanic glass (>20–25% modal). Modal analyses of the crystals gave averages of ~80–85% plagioclase, ~15–20% clinopyroxene, and small amounts of Fe-Ti oxide minerals. These mineralogical characteristics permitted the classification of the investigated rocks as basalts. The investigated rock samples were characterized by radiating arrays of fibrous, acicular plagioclase crystals in a glassy material, giving rise to a spherulitic texture (Figure 2c). A trachytic-like texture composed of a semi-fluidal fabric where tabular plagioclase grains were aligned in a subparallel mode was also observed (Figure 2d). Our thin-section observations showed that plagioclase formed small (<0.1 mm) to large (~0.5 mm) subhedral to

ehedral laths. Clinopyroxene grains are smaller than 0.5 mm anhedral to subhedral, with a weak pleochroism. Oxide minerals mainly occur as small (<50 μm) globular- to irregular-shaped inclusions in clinopyroxene and plagioclase (Figure 2c). Plagioclase is commonly replaced by calcite and zeolites, and clinopyroxene is pseudomorphically replaced by a mixture of clay minerals, oxyhydroxides, and calcite. The volcanic glass is unaltered, but in places, it can be devitrified to a greenish assemblage composed of clay and zeolites.

4. Methods and Results

4.1. Analytical Methods

Eight basalt samples were selected for bulk rock analyses of major element oxides and trace elements. Seven of those basalts samples were analyzed for their Sr–Nd–Hf isotopes. Details of all the analytical procedures are provided in the Supplementary Materials file. Results of the whole-rock and isotope analyses of the investigated rocks are given in the Supplementary Table S1.

4.2. Results

4.2.1. Major and Trace Element Analysis

Our thin-section observations showed that the basalt samples from the WPB were not significantly affected by post-solidification alterations. This observation was consistent with their low loss on ignition (LOI) values (1.30–1.70 wt%). The compositions of the basalt samples from the WPB varied shortly in: SiO_2 (48.10–49.20 wt%), Al_2O_3 (16.18–16.69 wt%), CaO (11.38–11.71 wt%), and MgO (4.15–4.90 wt%). This suggests that the investigated basalts collectively comprised a geochemically homogeneous group of mafic rocks. In addition, the values of the magnesium number (Mg\# : $100 \times \text{Mg}/(\text{Mg} + \text{Fe}^{2+})$) for the basalts of the WPB ranged from 44 to 50.

On the $(\text{Na}_2\text{O} + \text{K}_2\text{O})$ vs. SiO_2 diagram [23], the basalts from the WPB showed an apparently subalkaline composition (Figure 3a). On the discrimination diagram V vs. $\text{Ti}/10^3$ [24], the investigated rock samples were plotted in the field of lavas with a mid-ocean ridge basalt (MORB)- and back-arc basin basalt (BABB)-like geochemical affinity (Figure 3b). We noted that the composition of the basalts from the WPB was like that of other basalt samples that have been collected from the study area in previous investigations.

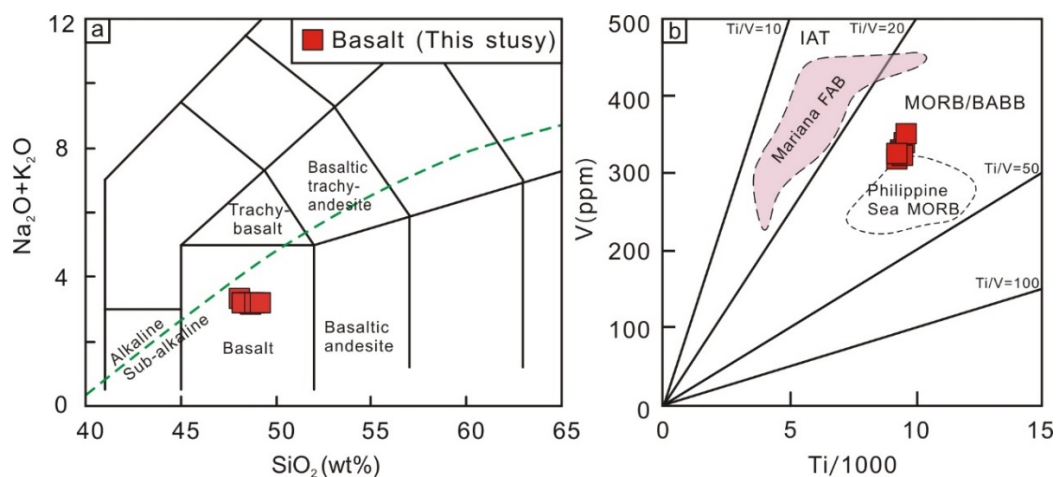


Figure 3. Geochemical diagrams of basalts from CBF in WPB: (a) SiO_2 vs. total alkalis ($\text{Na}_2\text{O} + \text{K}_2\text{O}$) diagram of Reference [23]. The alkaline–subalkaline boundary is from Reference [25]. (b) The V vs. $\text{Ti}/10^3$ diagram is from Reference [24]. The Marianna FAB are from Reference [26], and the Philippine Sea MORB are from References [4–9]. Abbreviations (in alphabetical order): BABB: back-arc basin basalt, FAB: fore-arc basalt, IAT: island arc tholeiite, and MORB: mid-ocean ridge basalt.

The total lanthanide contents of the basalt samples from the WPB vary between 41.3 and 45.4 ppm. Basalts display chondrite-normalized lanthanide patterns that are characterized by slight depletions in the light lanthanides and nearly flat Eu to Lu segments

(Figure 4a). The MORB-normalized multielement patterns of the investigated basalts display depletions in Nb and marked enrichments in Ba, U, Pb, and Sr (Figure 4b). These enrichments in Ba and U are probably due to minor seafloor alterations. Moreover, a few basalt samples from the WPB show mild negative anomalies in Nd and Ti and positive anomalies in Zr and Hf.

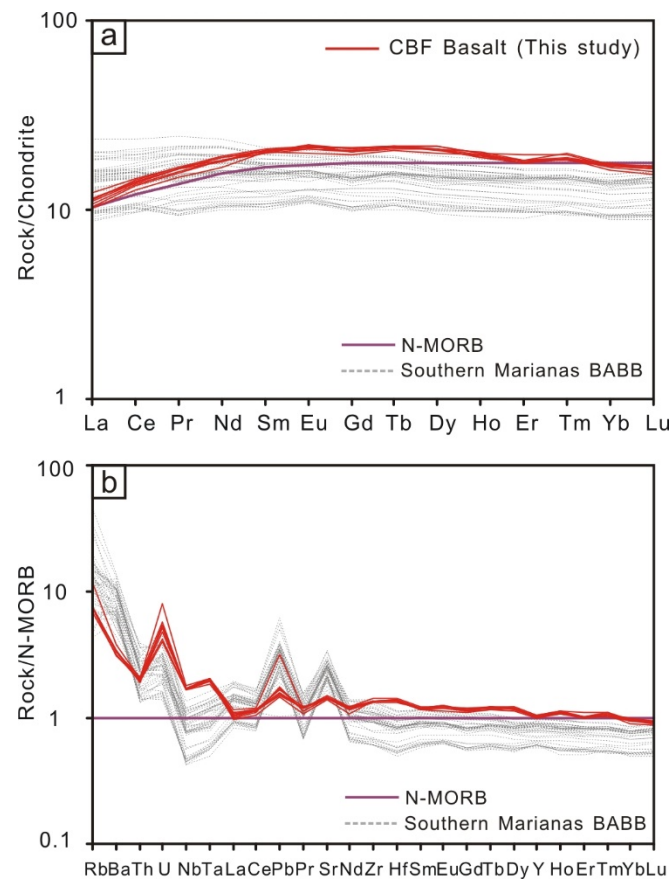


Figure 4. (a) Chondrite-normalized lanthanide profiles and (b) N-MORB-normalized trace element profiles for basalts from CBF in the WPB. The chondrite- and N-MORB-normalizing data are from Reference [27]. Data for the Southern Mariana back-arc basin are from Reference [28].

4.2.2. Sr–Nd–Hf Isotope Systematics

The Rb contents of basalts from the WPB show an antagonistic correlation with their Mg# values (not shown here). This suggests that Rb was most likely not mobilized during the oceanic alteration. As such, the initial $^{87}\text{Sr}/^{86}\text{Sr}$ (hereafter $^{87}\text{Sr}/^{86}\text{Sr}_i$) ratios measured in the basalts from the study area were accurate. The basalt samples from the WPB had $^{87}\text{Sr}/^{86}\text{Sr}_i$ ratios of 0.703339–0.703455 and initial $^{143}\text{Nd}/^{144}\text{Nd}$ ratios (herein $^{143}\text{Nd}/^{144}\text{Nd}_i$) of 0.513050–0.513089. Furthermore, they showed $\epsilon_{\text{Nd}}(t)$ values of 8.0–8.7. On the $\epsilon_{\text{Nd}}(t)$ vs. $^{87}\text{Sr}/^{86}\text{Sr}_i$ binary diagram, the isotopic signatures of the investigated basalts are plotted in the field of mafic rocks with a MORB-like geochemical affinity (Figure 5a).

Basalts from the WPB have $^{176}\text{Hf}/^{177}\text{Hf}$ ratios that range from 0.28318 to 0.28321, corresponding to $\epsilon_{\text{Hf}}(t)$ from 15.2 to 16.3. Although several different Indian–Pacific boundaries in the Hf–Nd space have been proposed, here, we used that of Reference [29] to define the mantle domains in the WPB (Figure 5b). All samples were plotted in the Indian Ocean compositional field (Figure 5b). In addition, our data defined a trend of plots in the compositional field of mafic lavas from the Mariana BAB (Figure 5b).

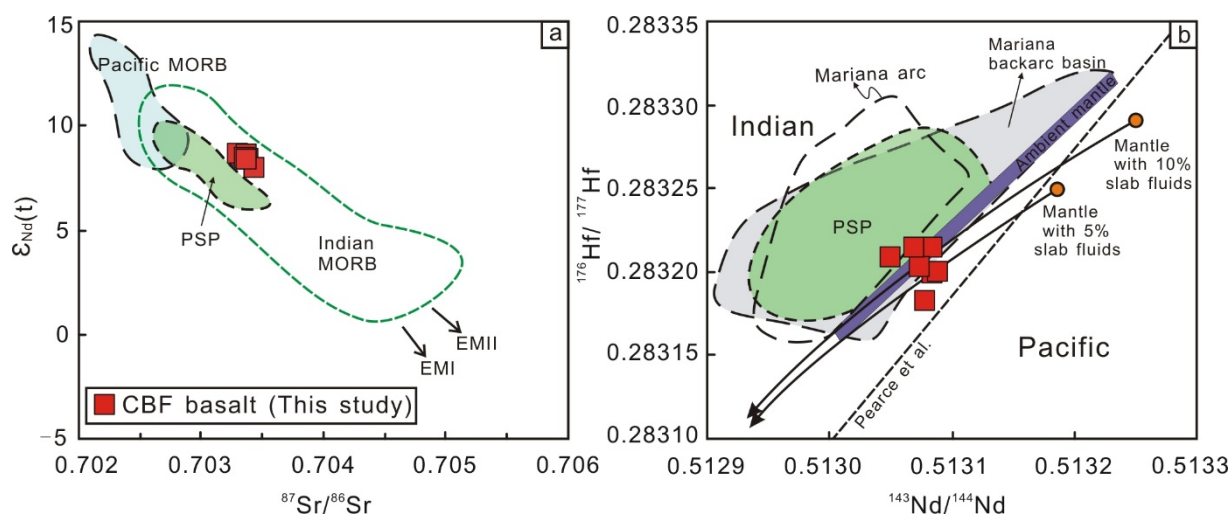


Figure 5. (a) Binary plot of $\epsilon_{\text{Nd}}(t)$ vs. $^{87}\text{Sr}/^{86}\text{Sr}(i)$ for basalts from CBF in the WPB (modified after Reference [30]). (b) Hf–Nd diagram (modified after References [27,31]) used to highlight the mantle heterogeneities beneath the WPB. The Hf–Nd isotopic composition of the investigated basalts is explained as a mixing array between the ambient mantle and a 60:40 bulk mixture between the subducted (altered) oceanic crust and overlying sediments (ODP, Site 801), as in Reference [32]. The red diamonds entitled “mantle with 10% slab fluids” and “mantle with 5% slab fluids” represent an averaged composition of a pre-subduction mantle (i.e., prior to any slab fluid addition). Data for the Mariana arc lavas are from References [33–35]. Data for the Mariana back-arc basin lavas are from References [36–38].

5. Discussion

5.1. Potential Effects of Post-Eruptive Alteration, Fractionation, and Assimilation

Our thin-section observations showed that basalts from the WPB were affected by post-magmatic alterations only to a minor extent. This was consistent with their low LOI values (1.30–1.70 wt %). As such, only elements that could not be significantly affected by post-solidification processes were used to infer conclusions about the petrogenesis of basalts from the WPB. These mostly included some incompatible trace elements such as Hf, Th, Y, Ta, Nb, and the lanthanides. The good correlations between these elements and the relatively immobile Zr (not shown here) implied that their concentrations were not disturbed by seafloor alterations.

Basalts from the WPB lack positive Eu anomalies in chondrite-normalized lanthanide patterns. This suggests that the formation of basalts was not controlled by cumulus processes, and thus, they represent liquid compositions.

A critical question is whether the formation of the parental melts of basalts from the WPB was affected by inputs of subducted continental materials. The Nb/La ratios of the basalts from the study area were too high (1.42–1.63) to be a result of assimilation of the continental crust (Nb/La < 1.01) [39]. Furthermore, the investigated basalts had much lower Th/Ta ratios than the continental crust (1.06–1.56 vs. ≥ 8 , respectively) [40]. As such, we conclude that the parental melts of basalts from the WPB were not modified by subducted continental components.

It is known that mantle-derived magmas may undergo contamination by the oceanic crust during ascent. Basalts from the WPB plot within the present day MORB–OIB array in the Th/Yb vs. Nb/Yb diagram (Figure 6a) [41] support the idea that they were generated at an oceanic setting due to a melt flux following near-free contamination pathways. Moreover, basalts from the WPB lack oceanic gabbro xenoliths and have much lower $\text{K}_2\text{O}/\text{P}_2\text{O}_5$ ratios (1.35–1.64) than those that have been affected by the assimilation of wall rock oceanic gabbro (≥ 4.7) [42].

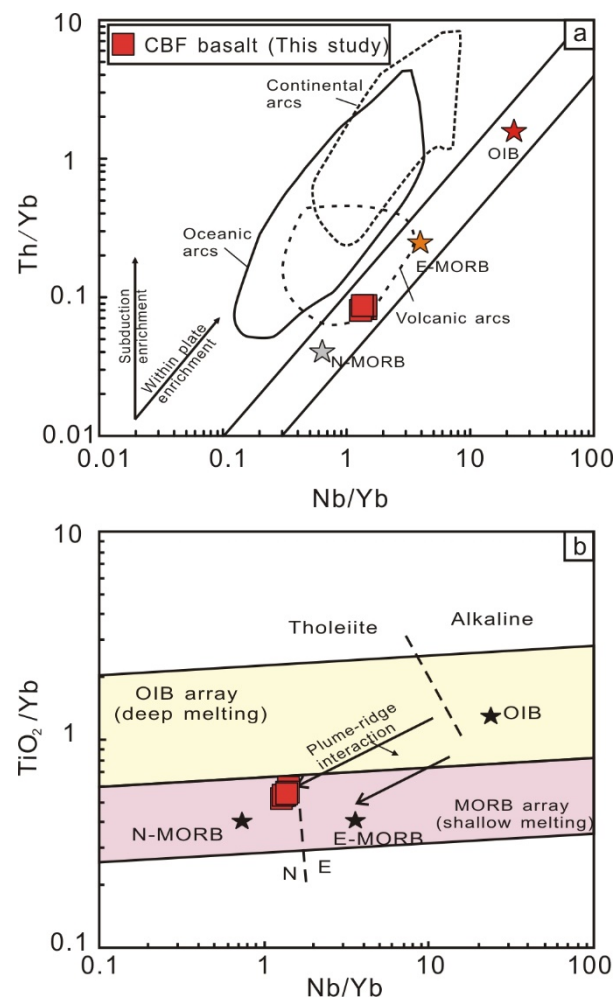


Figure 6. (a) Th/Yb vs. Nb/Yb and (b) TiO₂/Yb vs. Nb/Yb discrimination diagrams for basalts from CBF in the WPB (modified after Reference [41]). (a) The compositional trends for subduction enrichment, crustal contamination, and within-plate enrichment are from Reference [41]. Abbreviations (in alphabetical order): E-MORB: enriched-type mid-ocean ridge basalt, N-MORB: normal-type mid-ocean ridge basalt, OIB: ocean island basalt, UM: upper mantle, Alk: alkaline, PM: primitive mantle, and Th: tholeiitic.

We concluded that the composition of basalts from the WPB was primarily controlled by magma differentiation. We noted that fractional crystallization cannot change the Sr–Nd isotope ratios of mafic melts. As such, the isotopic composition of basalts can also help us understand their petrogenesis.

5.2. Source of Basalts from the WPB and Melting Conditions

Insights into the depth of melting of the mantle source of basalts from the WPB can be obtained by semiquantitative trace element modeling. On the TiO₂/Yb vs. Nb/Yb discrimination diagram (Figure 6b), basalts from the WPB plot in the shallow melting array showed a similar composition to that of tholeiites derived from melting of a depleted MORB mantle (DMM). In addition, the compositions of basalts from the study area straddled the boundary between the fields of the MORB and enriched-type mid-ocean ridge basalt (E-MORB; Figure 6b), implying that they originated from an enriched lithospheric mantle (EM) source. This indicates that the parental melt of basalts from the WPB were generated at much shallower depths than those of typical plume-derived basalts [43]. Alternatively, the parental melts of the investigated basalts could not have been formed by the melting of a mantle region that was influenced by OIB-type components, consistent with the compositional data.

Determining that the mantle source lithology of basalts from the WPB is vital for understanding the formation of magma and modeling of compositional data, it is expected that melts derived from the melting of garnet peridotite will display chondrite-normalized lanthanide diagrams characterized by a high fractionation of the heavy lanthanides [44], whereas melts generated by the low-degree melting of garnet peridotite will show depletion in the light lanthanides [45]. To practically test the reliability of this theoretical assumption, we applied a nonmodal, batch partial melting model using La/Yb vs. Dy/Yb ratio plots (Figure 7a) [46]. The compositions of basalts from the WPB cannot be explained by melting in the garnet peridotite stability field. On the contrary, they can be reproduced by ~20% melting of a spinel-bearing peridotite source (S2; Figure 7a). We also estimated the degree of melting required for the formation of the parental melts of basalts from the WPB using the Sm/Yb vs. Sm discrimination diagrams (Figure 7b) [41,47]. This plot also shows that the parental melts of the investigated basalts were most likely produced by ~20% decompression melting of a rising spinel-bearing peridotite source.

5.3. Insights into the Origin of Basalts from the WPB

The petrogenesis of basalts from the WPB has been the subject of many frontline studies and remains a hotly debated issue among geologists, many of whom passionately defend ideas about their origin. Previous studies have interpreted mafic volcanics from the study area as: (i) OIB-type lithologies [3,11,12] and (ii) N-MORB- [1,2,4] and (iii) BAB-type mafic rocks [7,31].

Compositional evidence suggests that a thermal plume may have played a significant role in the formation of the seamounts of the Benham Rise in the WPB during the Eocene [4,8,11,12]; our samples and data show its influence did not extend to the study area. A source enrichment by OIB-like melts or veins would not be consistent with the trace element patterns of basalts from the WPB (Figure 4b). Furthermore, there is no significant isotopic difference between samples with high and low Th, Nb, Ta, and light lanthanide contents. It is likely that these compositional differences are linked to sub-ridge partial melting processes [54].

Based on their geochemical signatures, basalts from the WPB are oceanic in origin. They could either be N-MOR basalts formed at a mature spreading center or BAB basalts with a small contribution of crustal materials derived from a downgoing oceanic lithospheric slab or even island arc tholeiitic (IAT) basalts. On the discrimination diagram V vs. Ti/10³ (Figure 3b), basalts from the study area were plotted out on the field of mafic rocks with an IAT-type affinity. When compared to fore-arc basalts (FAB) from the Mariana trough, basalts from the WPB are compositionally different as well. In fact, the investigated basalts were plotted in the field of lavas with a MOR- and BAB-like geochemical affinities. Even though most basalts from the WPB erupted at a depth of more than 5 km, they are vesicular in structure. We note that MOR-type basalts are typically not vesicular. Nevertheless, it is likely for BAB basalts to have a porous structure [7]. This suggests that basalts collected from the study area were most likely generated at a BAB setting.

The BAB-type basalts from the WPB have relatively high abundances of high-field strength elements (HFSE; i.e., Ti, Zr, and Hf). This implies that the investigated basalts were most likely derived from low degrees of melting of a fertile mantle source or from remelting of a relatively depleted mantle region metasomatized by slab-related components to some extent. As such, both possibilities are considered in the following discussion.

Due to the apparent immobility of Hf in slab-derived fluids [29], we used the Hf isotopes to see through the subduction signal and determine whether the inferred mantle source for the investigated basalts was Indian or Pacific in petrological nature. Covariations of ¹⁴³Nd/¹⁴⁴Nd and ¹⁷⁶Hf/¹⁷⁷Hf isotopic ratios (Figure 5b) indicate that the isotopic compositions of basalts from the WPB shift away from the averaged composition of a pre-subduction (ambient) mantle. This can be explained as due to the involvement of subduction components. This will drive the original composition of the mantle to lower Nd and Hf isotopic ratios, so that the ensuing basalts will be plotted in the field of an

Indian-type mantle. Indeed, all basalt samples were plotted in the Indian Ocean domain on the $^{176}\text{Hf}/^{177}\text{Hf}$ vs. $^{143}\text{Nd}/^{144}\text{Nd}$ isotope diagram of Reference [29] (Figure 5b).

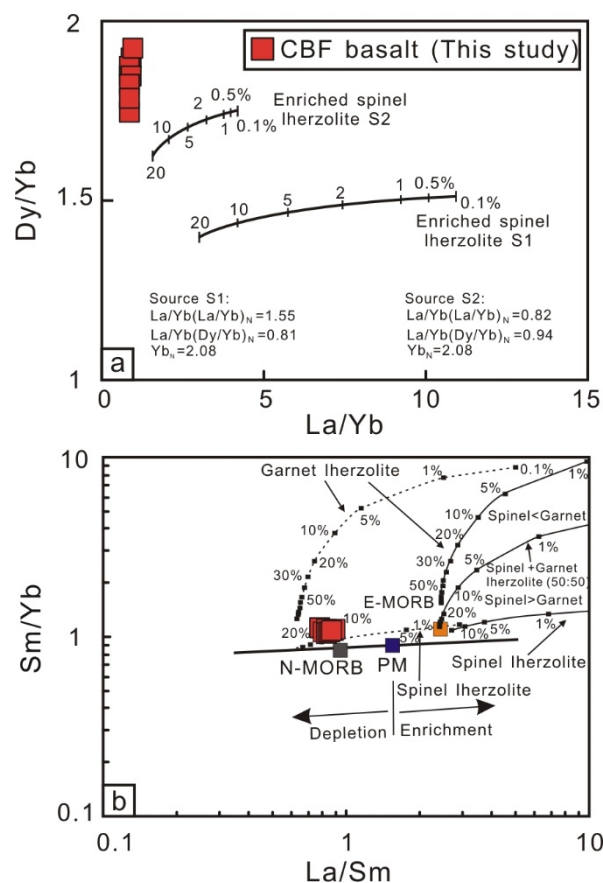


Figure 7. (a) La/Yb vs. Dy/Yb discrimination diagrams for basalts from CBF in the WPB (modified after Reference [48]). Melt curve models based on La/Yb vs. Dy/Yb are calculated using nonmodal, batch melts of garnet (gt) and spinel (sp) lherzolites for two different enriched mantle source compositions: S1 from Reference [49] and S2 from Reference [50]. (i) Melt curves for S1 and S2 in the spinel-facies; (ii) melt curves for S1 and S2 in both garnet- and spinel-peridotite-facies. Arrays representing mixing between various proportions of melt fractions from the garnet-facies mantle and melt fractions from the spinel-facies mantle are also shown. The garnet lherzolite mode is: 0.598 ol, 0.211 opx, 0.076 cpx, and 0.115 gt that melts in proportions of 0.04 ol, -0.19 opx, 1.04 cpx, and 0.11 gt. The spinel lherzolite mode is: 0.578 ol, 0.270 opx, 0.119 cpx, and 0.033 sp that melts in proportions of -0.06 ol, 0.28 opx, 0.67 cpx, and 0.11 sp. The mantle modes and melting proportions are from Reference [51]. The distribution coefficients are from Reference [52] for orthopyroxene and clinopyroxene and from Reference [53] for olivine, spinel, and garnet. The normalizing values are from Reference [27]. (b) The Sm/Yb vs. La/Sm discrimination diagram for basalt from the WPB (from Reference [47]). Numbers on the curves denote the degree of partial melting. The melting curves for spinel lherzolite ($\text{ol}_{53} + \text{opx}_{27} + \text{cpx}_{17} + \text{sp}_{11}$) and garnet peridotite ($\text{ol}_{60} + \text{opx}_{20} + \text{cpx}_{10} + \text{gt}_{10}$), enriched-type mid-ocean ridge basalt (E-MORB), normal-type mid-ocean ridge basalt (N-MORB), and primitive mantle (PM) compositions are from Reference [27]. Abbreviations (in alphabetical order): E-MORB: enriched-type mid-ocean ridge basalt, N-MORB: normal-type mid-ocean ridge basalt, and PM: primitive mantle.

On the same diagram, our analyses of basalts from the WPB defined a compositional trend on the lowermost side of the field of modern BAB lavas from the Mariana trough (Figure 5b). This suggests that the isotopic ratios of basalts from the study area resulted from the melting of a mantle source that was enriched by slab-related components to variable extents (<5% to >10%). This is consistent with the mixing of a mantle with a (clay-

rich or siliceous) sediment melt of a low Hf/Nd ratio and/or with an OIB-type source. On the Ba/Nb vs. Th/Nb diagram, basalts from the WPB were plotted in the overlapping area between the fields of MOR basalts and BAB lavas from the Mariana trough (Figure 8). From this diagram, it becomes apparent that trace element constraints favor a slight mixing of the mantle source with a sediment melt (Figure 8). This process can more effectively explain the low Hf/Nd ratios of the investigated basalts [31,32]. We conclude that a small amount of slab-derived sediment melt (from the subducted MORB-like PSP) was incorporated into the mafic melts produced by melting of the Indian-type mantle source below the WPB.

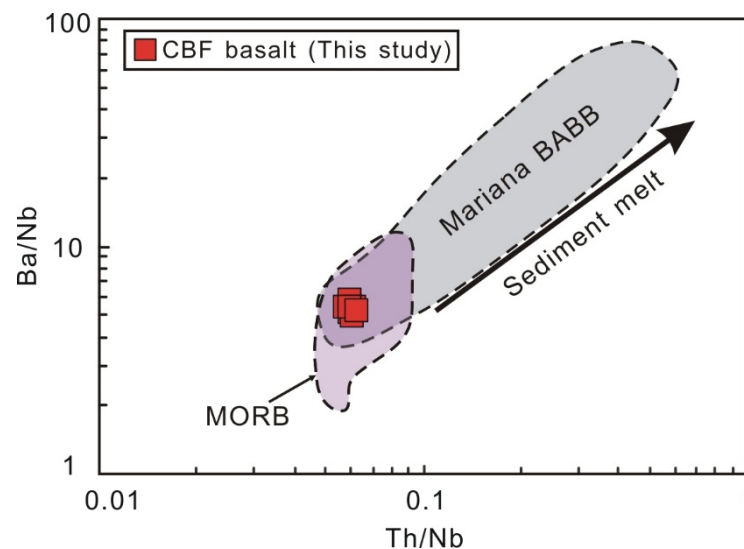


Figure 8. Ba/Nb vs. Th/Nb diagram [55] for basalts from CBF in the WPB.

5.4. Geotectonic Setting of the WPB

Tectonic reconstructions of the Philippine Sea Plate place the WPB in an oceanic setting at ~50 Ma, but the exact nature of this geotectonic setting is not well-understood yet. Questions about the origin and the geological evolution of the WPB remain largely unresolved. Submersible observations suggest that the WPB is a large piece of oceanic lithosphere (of the North New Guinea–Pacific) with a non-transform offset, fracture zones, a nodal deep, and an inside corner high [7,13]. Nevertheless, several tectonic and geophysical characteristics (i.e., the obliqueness of the trough and ridge structures and heat flow values) set the WPB apart from typical MOR environments, indicating that it underwent multiple phases of oceanic spreading. Furthermore, the Sr–Nd–Hf isotopic signatures of basalts from the WPB indicate an Indian Ocean MORB-like composition, suggesting that the WPB tapped an upper mantle region that was isotopically different from that beneath the spreading ridges of the Pacific [8].

A more conceptual model described the WPB as a BAB that opened between two active subduction zones and was progressively rotated clockwise [14,15]. In compositional terms, this geotectonic model could be tested by examining basalts from the study area for their geochemical affinity. Indeed, the BABB-like affinity of the mafic volcanic rock samples from the WPB strengthens the idea of their petrogenesis in a BAB setting [7]. Consequently, the question arises as to whether a BAB environment can explain the Indian-type isotopic signature of the mantle source of basalts from the study area.

It is known that a spatial relationship exists between subduction zones and the boundaries of isotopically different mantle domains. The Western Pacific BAB (i.e., Mariana trough and Lau Basin) produce basalts with Indian-type compositional signatures [56]. This suggests that the subducting PSP isolates the Indian and Pacific mantle sources with some apparent asthenospheric “leakage” along the transform fault zones and slab tears or gaps [41]. Based on the compositional evidence, it is unlikely that local subduction of the Pacific lithospheric plate or Western Pacific mantle plumes produced the Indian-type

signature in basalts from the WPB [5] (Figure 5b). Our interpretation is consistent with geophysical data indicating shrinking of the PSP owing to asthenospheric outflow around the subducted slab edges [31].

We emphasized the formation of the upper mantle of the PSP as part of a growing Indian-type mantle domain that spread into a broad area between Australia and Southeast Asia during much of the Cenozoic eon [5]. This type of heterogeneous mantle formed when the asthenosphere was variably contaminated by the heads of small-scale, ancient thermal plumes) or a large but diffuse old mantle diapir [9,57]. This is also consistent with the broad range in the isotopic compositions of basalts from the study area, implying the occurrence of heterogeneities in the mantle beneath the WPB at a cm-to-dm scale.

6. Conclusions

The principal findings of this investigation are the following:

- (1) Basalts from the WPB have trace element signatures typical of the BABB.
- (2) Their Sr–Nd–Hf isotopic characteristics are like those of Indian-type mafic rocks.
- (3) Geochemical modeling shows that they originated from ~20% melting of a N-MORB-like mantle source in the spinel peridotite stability field.
- (4) Depletions in Ti and Nd and low Hf/Sm ratios suggest that the mantle source of basalts from the study area incorporated a small amount of slab-derived sediment melt from the subducted PSP.
- (5) The compositional characteristics of basalts from the WPB indicate that their parental melts were formed at a BAB setting.

Supplementary Materials: The following are available online at <https://www.mdpi.com/article/10.3390/min11111277/s1>, Analytical methods: Details of the analytical procedures for the major and trace element and isotope analyses. Table S1: Results of the whole-rock and isotope analyses of the CBF basalts.

Author Contributions: Conceptualization, Z.Y., W.W. and L.C.; Formal Analysis, Z.Y., W.W. and L.C.; Investigation, Z.Y., W.W., L.C., Z.L., Q.L. and A.X.; Data Curation, Z.Y., W.W. and L.C.; Writing—Original Draft Preparation, Z.Y., W.W. and L.C.; Writing—Review and Editing, Z.Y., W.W., L.C., Z.L., Q.L. and A.X.; Visualization, Z.Y., Z.L., Q.L. and A.X. and Funding Acquisition, Z.Y. and W.W. All authors have read and agreed to the published version of the manuscript.

Funding: This work was financially supported by the National Natural Science Foundation of China (NNSFC; grant No. 41706055).

Acknowledgments: We would like to express our sincere gratitude to the personnel of the Wuhan Sample Solution Analytical Technology (WSSAT) Co., Wuhan (China) for their help at the stage of the geochemical and isotopic analyses of our samples.

Conflicts of Interest: The authors declare no conflict of interest. The funding sponsors had no role in the design of the study; in the collection, analyses, or interpretation of the data; in the writing of the manuscript; or in the decision to publish the results.

References

1. Marsh, N.G.; Saunders, A.D.; Tarney, J.; Dick, H.J.B. Geochemistry of basalts from the Shikoku and Daito basins, Deep Sea Drilling Project Leg 58. *Init. Rep. Deep Sea Drill. Proj.* **1980**, *58*, 805–842.
2. Matthey, D.P.; Marsh, N.G.; Tarney, J. The geochemistry, mineralogy and petrology of basalts from the West Philippine and Parece Vela Basins and from the Palau-Kyushu and West Mariana Ridges, Deep Sea Drilling Project Leg 59. *Initial Rep. Deep Sea Drill. Progr. Leg* **1981**, *59*, 753–797.
3. Miyashiro, A. Hot regions and the origin of marginal basins in the western Pacific. *Tectonophysics* **1986**, *122*, 122–216. [[CrossRef](#)]
4. Hickey-Vargas, R. Isotope characteristics of submarine lavas from the Philippine Sea: Implications for the origin of arc and basin magmas of the Philippine tectonic plate. *Earth Planet. Sci. Lett.* **1991**, *107*, 290–304. [[CrossRef](#)]
5. Hickey-Vargas, R. Origin of the Indian Ocean-type isotopic signature in basalts from Philippine Sea plate spreading centers: An assessment of local versus large-scale processes. *J. Geophys. Res. Solid Earth* **1998**, *103*, 20963–20980. [[CrossRef](#)]
6. Hickey-Vargas, R. Basalt and tonalite from the Amami Plateau, northern West Philippine Basin: New Early Cretaceous ages and geochemical results, and their petrologic and tectonic implications. *Isl. Arc.* **2005**, *14*, 653–665. [[CrossRef](#)]

7. Fujioka, K.; Okino, K.; Kanamatsu, T.; Ohara, Y.; Ishizuka, O.; Haraguchi, S.; Ishii, T. Enigmatic extinct spreading center in the West Philippine backarc basin unveiled. *Geology* **1999**, *27*, 1135–1138. [[CrossRef](#)]
8. Savov, I.P.; Hickey-Vargas, R.; D'Antonio, M.; Ryan, J.G.; Spadea, P. Petrology and geochemistry of West Philippine Basin basalts and early Palau–Kyushu arc volcanic clasts from ODP Leg 195, Site 1201D: Implications for the early history of the Izu–Bonin–Mariana Arc. *J. Petrol.* **2006**, *47*, 277–299. [[CrossRef](#)]
9. Hickey-Vargas, R.; Bizimis, M.; Deschamps, A. Onset of the Indian Ocean isotopic signature in the Philippine Sea Plate: Hf and Pb isotope evidence from Early Cretaceous terranes. *Earth Planet. Sci. Lett.* **2008**, *268*, 255–267. [[CrossRef](#)]
10. Ishizuka, O.; Taylor, R.N.; Ohara, Y.; Yuasa, M. Upwelling, rifting, and age-progressive magmatism from the Oki-Daito mantle plume. *Geology* **2013**, *41*, 1011–1014. [[CrossRef](#)]
11. Wang, R.R.; Yan, Q.S.; Tian, L.Y.; Zhang, H.T.; Shi, M.J. Magmatic conditions of basaltic rocks from the Benham Rise in the West Philippine Basin and its geological significances. *Adv. Mar. Sci.* **2018**, *36*, 229–240.
12. Yuan, L.; Yan, Q.S.; Liu, Y.G.; Wu, S.Y.; Wang, R.R.; Shi, X.F. In situ geochemical compositions of the minerals in basaltic rocks from the West Philippine Basin: Constraints on source lithology and magmatic processes. *Lithosphere* **2020**, *1*, 8878501. [[CrossRef](#)]
13. Hilde, T.W.C.; Lee, C.-S. Origin and evolution of the West Philippine Basin: A new interpretation. *Tectonophysics* **1984**, *102*, 85–104. [[CrossRef](#)]
14. Hall, R.; Fuller, M.; Ali, J.R.; Anderson, C.D. The Philippine Sea Plate: Magnetism and reconstructions. In *Active Margins and Marginal Basins of the Western Pacific*; Taylor, B., Natland, J., Eds.; AGU: Washington, DC, USA, 1995; pp. 371–404. [[CrossRef](#)]
15. Tan, H.Y.; Wang, Z. Seismic velocity imaging and tectonic characteristics of bidirectional subducting slabs under Philippine Archipelago. *Chin. J. Geophys.* **2018**, *61*, 4887–4990.
16. Hall, R. Cenozoic geological and plate tectonic evolution of SE Asia and the SW Pacific: Computer-based reconstructions, model and animations. *J. Asian Earth Sci.* **2002**, *20*, 353–431. [[CrossRef](#)]
17. Xia, C.L.; Zheng, Y.P.; Dong, D.D.; Qu, H.B.; Zhang, X.X.; Li, X.F.; Hua, Q.F. Characteristics of magnetic lineations and reconstruction of seafloor spreading processes of the Philippine Sea Basin since 61 Ma. *Mar. Geol. Quat. Geol.* **2017**, *37*, 30–40.
18. Wu, J.; Suppe, J.; Lu, R.; Kanda, R. Philippine Sea and East Asian plate tectonics since 52 Ma constrained by new subducted slab reconstruction methods. *J. Geophys. Res. Solid Earth* **2016**, *121*, 4670–4741. [[CrossRef](#)]
19. Sato, T.; No, T.; Kodaira, S.; Takahashi, N.; Kaneda, Y. Seismic constraints of the formation process on the back-arc basin in the southeastern Japan Sea. *J. Geophys. Res.* **2014**, *229*, 1563–1579. [[CrossRef](#)]
20. Uyeda, S.; Ben-Avraham, Z. Origin and development of the Philippine Sea. *Nat. Phys. Sci.* **1972**, *240*, 176–178. [[CrossRef](#)]
21. Seno, T.; Maruyama, S. Paleogeographic reconstruction and origin of the Philippine Sea. *Tectonophysics* **1984**, *102*, 53–84. [[CrossRef](#)]
22. Deschamps, A.; Lallemand, S. The West Philippine Basin: An Eocene to early Oligocene back arc basin opened between two opposed subduction zones. *J. Geophys. Res.* **2002**, *107*, 2322. [[CrossRef](#)]
23. Le Bas, M.J.; Le Maitre, R.W.; Streckeisen, A.; Zanettin, B.A. Chemical classification of volcanic rocks based on the total alkalisilica diagram. *J. Petrol.* **1986**, *27*, 745–750. [[CrossRef](#)]
24. Shervais, J.W. Ti-V plots and the petrogenesis of modern and ophiolitic lavas. *Earth Planet. Sci. Lett.* **1982**, *59*, 101–118. [[CrossRef](#)]
25. Irvine, T.N.; Baragar, W.R.A. A Guide to the Chemical Classification of the Common Volcanic Rocks. *Can. J. Earth Sci.* **1971**, *8*, 523–548. [[CrossRef](#)]
26. Reagan, M.K.; Ishizuka, O.; Stern, R.J.; Kelley, K.A.; Ohara, Y.; Blichert-Toft, J.; Bloomer, S.H.; Cash, J.; Fryer, P.; Hanan, B.B.; et al. Fore-arc basalts and subduction initiation in the Izu–Bonin–Mariana system. *Geochem. Geophys. Geosyst.* **2010**, *11*. [[CrossRef](#)]
27. Sun, S.S.; McDonough, W.F. Chemical and isotopic systematics of ocean basalt: Implications for mantle composition and processes. *Geol. Soc. Lond. Spec. Publ.* **1989**, *42*, 313–345. [[CrossRef](#)]
28. Ribeiro, J.M.; Stern, R.J.; Kelley, K.A.; Martinez, F.; Ishizuka, O.; Manton, W.I.; Ohara, Y. Nature and distribution of slab-derived fluids and mantle sources beneath the Southeast Mariana forearc rift. *Geochem. Geophys. Geosyst.* **2013**, *14*, 4585–4607. [[CrossRef](#)]
29. Pearce, J.A.; Kempton, P.D.; Nowell, G.M.; Noble, S.R. Hf–Nd element and iso-tope perspective on the nature and provenance of mantle and subduction components in western Pacific arc-basin systems. *J. Petrol.* **1999**, *40*, 1579–1611. [[CrossRef](#)]
30. Zindler, A.; Hart, S. Chemical geodynamics. *Annu. Rev. Earth Planet. Sci.* **1986**, *14*, 493–571. [[CrossRef](#)]
31. Ribeiro, J.M.; Stern, R.J.; Martinez, F.; Woodhead, J.; Chen, M.; Ohara, Y. Asthenospheric outflow from the shrinking Philippine Sea Plate: Evidence from Hf–Nd isotopes of southern Mariana lavas. *Earth Planet. Sci. Lett.* **2017**, *478*, 258–271. [[CrossRef](#)]
32. Woodhead, J.D.; Stern, R.J.; Pearce, J.A.; Hergt, J.M.; Vervoort, J. Hf–Nd isotope variation in Mariana Trough basalts: The importance of “ambient mantle” in the interpretation of subduction zone magmas. *Geology* **2012**, *40*, 539–542. [[CrossRef](#)]
33. Stern, R.J.; Kohut, E.; Bloomer, S.H.; Leybourne, M.; Fouch, M.; Vervoort, J. Subduction factory processes beneath the Guguan cross-chain, Mariana Arc: No role for sediments, are serpentinites important? *Contrib. Mineral. Petrol.* **2006**, *151*, 202–221. [[CrossRef](#)]
34. Wade, J.A.; Plank, T.; Stern, R.J.; Tollstrup, D.L.; Gill, J.B.; O’Leary, J.C.; Eiler, J.M.; Moore, R.B.; Woodhead, J.D.; Trusdell, F.; et al. The May 2003 eruption of Anatahan volcano, Mariana Islands: Geochemical evolution of a silicic island-arc volcano. *J. Volcanol. Geotherm. Res.* **2005**, *146*, 139–170. [[CrossRef](#)]
35. Woodhead, J.D. Geochemistry of the Mariana arc (Western Pacific): Source composition and processes. *Chem. Geol.* **1989**, *76*, 1–24. [[CrossRef](#)]
36. Gribble, R.F.; Stern, R.J.; Bloomer, S.H.; Stüben, D.; O’Hearn, T.; Newman, S. MORB mantle and subduction components interact to generate basalts in the southern Mariana Trough backarc basin. *Geochim. Cosmochim. Acta* **1996**, *60*, 2153–2166. [[CrossRef](#)]

37. Gribble, R.F.; Stern, R.J.; Newman, S.; Bloomer, S.H.; O'Hearn, T. Chemical and Isotopic Composition of Lavas from the Northern Mariana Trough: Implications for Magmagenesis in Backarc Basins. *J. Petrol.* **1998**, *39*, 125–154. [[CrossRef](#)]
38. Volpe, A.M.; Douglas Macdougall, J.; Lugmair, G.W.; Hawkins, J.W.; Lonsdale, P.F. Fine-scale isotopic variation in Mariana Trough basalts: Evidence for heterogeneity and a recycled component in backarc basin mantle. *Earth Planet. Sci. Lett.* **1990**, *100*, 251–264. [[CrossRef](#)]
39. Kieffer, B.; Arndt, N.; Lapierre, H.; Bastien, F.; Bosch, D.; Pecher, A.; Yirgu, G.; Ayalew, D.; Weis, D.; Jerram, D.A.; et al. Flood and shield basalts from Ethiopia: Magmas from the African superswell. *J. Petrol.* **2004**, *45*, 793–834. [[CrossRef](#)]
40. Rudnick, R.L.; Gao, S. The Composition of the Continental Crust. In *The Crust*; Holland, H.D., Turekian, K.K., Eds.; Treatise on Geochemistry; Elsevier-Pergamon: Oxford, UK, 2003; Volume 3, pp. 1–64.
41. Pearce, J.A. Geochemical fingerprinting of oceanic basalts with applications to ophiolite classification and the search for Archean oceanic crust. *Lithos* **2008**, *100*, 14–48. [[CrossRef](#)]
42. Borisova, A.Y.; Faure, F.; Deloule, E.; Grégoire, M.; Béjina, F.; Parseval, D.P.; Devidal, J.-L. Lead isotope signatures of Kerguelen plume-derived olivine-hosted melt inclusions: Constraints on the ocean island basalt petrogenesis. *Lithos* **2014**, *198*, 153–171. [[CrossRef](#)]
43. Putirka, K. Clinopyroxene-liquid equilibria to 100 kbar and 2450 K. *Contrib. Mineral. Petrol.* **1999**, *135*, 151–163. [[CrossRef](#)]
44. Workman, R.K.; Hart, S.R. Major and trace element composition of the depleted MORB mantle (DMM). *Earth Planet. Sci. Lett.* **2005**, *231*, 53–72. [[CrossRef](#)]
45. Niu, Y.; Regelous, M.; Wendt, I.J.; Batiza, R.; O'Hara, M.J. Geochemistry of near-EPR seamounts: Importance of source vs. process and the origin of enriched mantle component. *Earth Planet. Sci. Lett.* **2002**, *199*, 327–345. [[CrossRef](#)]
46. Thirlwall, M.F.; Smith, T.E.; Graham, A.M.; Theodorou, N.; Hollings, P.; Davidson, J.P.; Arculus, R.J. High field strength element anomalies in arc lavas: Source or process. *J. Petrol.* **1994**, *35*, 819–838. [[CrossRef](#)]
47. Aldanmaz, E.; Pearce, J.A.; Thirlwall, M.F.; Mitchell, J.G. Petrogenetic evolution of late Cenozoic, post-collision volcanism in western Anatolia, Turkey. *J. Volcanol. Geotherm. Res.* **2000**, *102*, 67–95. [[CrossRef](#)]
48. Saccani, E.; Allahyari, K.; Rahimzadeh, B. Petrology and geochemistry of mafic magmatic rocks from the Sarve-Abad ophiolites (Kurdistan region, Iran): Evidence for interaction between MORB-type asthenosphere and OIB-type components in the southern Neo-Tethys Ocean. *Tectonophysics* **2014**, *621*, 132–147. [[CrossRef](#)]
49. Saccani, E.; Allahyari, K.; Beccaluva, L.; Bianchini, G. Geochemistry and petrology of the Kermanshah ophiolite (Iran): Implication for the interaction between passive rifting, oceanic accretion, and OIB-type components in the Southern Neo-Tethys Ocean. *Gondwana Res.* **2013**, *24*, 392–411. [[CrossRef](#)]
50. Saccani, E.; Azimzadeh, Z.; Dilek, Y.; Jahangiri, A. Geochronology and petrology of the early carboniferous Misho Mafic Complex (NW Iran), and implications for the melt evolution of Paleo-Tethyan rifting in Western Cimmeria. *Lithos* **2013**, *162–163*, 264–278. [[CrossRef](#)]
51. Kinzler, R.J. Melting of mantle peridotite at pressures approaching the spinel to garnet transition: Application to mid-ocean ridge basalt petrogenesis. *J. Geophys. Res. Solid Earth* **1997**, *102*, 853–874. [[CrossRef](#)]
52. Irving, A.J.; Frey, F.A. Trace element abundances in megacrysts and their host basalts: Constraints on partition coefficients and megacryst genesis. *Geochim. Cosmochim. Acta* **1984**, *48*, 1201–1221. [[CrossRef](#)]
53. McKenzie, D.; O'Nions, R.K. Partial melt distributions from inversion of rare earth element concentrations. *J. Petrol.* **1991**, *32*, 1021–1091. [[CrossRef](#)]
54. Langmuir, C.H.; Klein, E.M.; Plank, T. Petrological systematics of mid-ocean ridge basalts: Constraints on melt generation beneath ocean ridges. In *Mantle Flow and Melt Generation at Mid-Ocean Ridges*, Geophysical Monograph 71; Morgan, J.P., Blackman, D.K., Sinton, J.M., Eds.; AGU: Washington, DC, USA, 1992; pp. 183–280.
55. Pearce, J.A.; Stern, R.J.; Bloomer, S.H.; Fryer, P. Geochemical mapping of the Mariana arc-basin system: Implications for the nature and distribution of sub-duction components. *Geochem. Geophys. Geosyst.* **2005**, *6*, 1–27. [[CrossRef](#)]
56. Hawkesworth, C.J.; Gallagher, K.; Hergt, J.M.; Mcdermott, F. Mantle and slab contributions in arc magmas. *Annu. Rev. Earth Planet. Sci.* **1993**, *21*, 175–204. [[CrossRef](#)]
57. Tu, K.; Flower, M.F.J.; Carlson, R.; Xie, G.; Chen, C.-Y.; Zhang, M. Magmatism in the South China Basin, 1, Isotopic and trace-element evidence for an endogenous Dupal mantle component. *Chem. Geol.* **1992**, *97*, 47–63. [[CrossRef](#)]